https://doi.org/10.5194/angeo-2021-27
Preprint. Discussion started: 24 June 2021

Annales Geophysicae Discussions

Seasonal features of geomagnetic activity: evidence for solar activity dependence?

Adriane Marques de Souza Franco[1], Rajkumar Hajra[2], Ezequiel Echer[1], and Mauricio José Alves Bolzan[3]

[1]Instituto Nacional de Pesquisas Espaciais (INPE), São José dos Campos, Brazil
[2]Indian Institute of Technology Indore, Simrol, Indore 453552, India
[3]Federal University of Jatai, Jatai, Brazil

Correspondence: Adriane Marques de Souza Franco (adrianemarquesds@gmail.com)

Abstract. Seasonal features of geomagnetic activity and their solar wind-interplanetary drivers are studied using more than 5 solar cycles of geomagnetic activity and solar wind observations. This study involves a total of 1239 geomagnetic storms of varying intensity identified using the Dst index from January 1963 to December 2019, a total of 75863 substorms identified from the SML index from January 1976 to December 2019, a total of 145 high-intensity long-duration continuous auroral electrojet (AE) activity (HILDCAA) events identified using the AE index from January 1975 to December 2017. The occurrence rates of the substorms, geomagnetic storms, including moderate (-50 nT $\geq$ Dst > -100 nT) and intense (-100 nT $\geq$ Dst > -250 nT), exhibit a significant semi-annual variation (periodicity ~ 6 months), while the super storms (Dst ≤ -250 nT) and HILDCAAs do not exhibit any clear seasonal feature. The geomagnetic activity indices Dst and ap exhibit a semi-annual variation while AE exhibits an annual variation (periodicity ~ 1 year). The annual and semi-annual variations are found to be driven by the annual variation of the solar wind speed V_{sw} and the semi-annual variation of the coupling function VB_s (where $V = V_{sw}$, and B_s is the southward component of the interplanetary magnetic field), respectively. We present a detailed analysis of the annual and semi-annual variations and their dependencies on the solar activity cycles separated as the odd, even, weak and strong solar cycles.

1 Introduction

Solar wind-magnetosphere energy coupling causes disturbances in the magnetosphere of the Earth (e.g., Dungey, 1961; Axford and Hines, 1961; Tsurutani et al., 1992; Gonzalez et al., 1994). Depending on the efficiency, strength and duration of the coupling, resultant geomagnetic disturbances (von Humboldt, 1808) can be classified as magnetic storms, substorms and high-intensity long-duration continuous auroral activities (HILDCAAs) (Gonzalez et al., 1994; Hajra, 2021b). In general, magnetic storms represent global-scale disturbances caused by enhancement in (westward) ring currents flowing at $\sim 2-7$ Earth radii ($R_\oplus$) in the magnetic equatorial plane of the Earth (Gonzalez et al., 1994; Lakhina and Tsurutani, 2018, and references therein). Storms can continue for a few hours to a day. Substorms (Akasofu, 1964) are shorter-scale, a few minutes to an hour, disturbances in the auroral region caused by precipitations of $\sim 10-100$ keV electrons and protons in the atmosphere. Intense auroral substorms continuing for a few days without occurrence of any major magnetic storms have been called HILDCAAs

https://doi.org/10.5194/angeo-2021-27
Preprint. Discussion started: 24 June 2021


Annales Geophysicae Discussions

(Tsurutani and Gonzalez, 1987; Hajra et al., 2013) to distinguish them from nominal substorms and major magnetic storms (Tsurutani et al., 2004; Guarnieri, 2006).

One of the earliest-reported features of the geomagnetic activity is the semi-annual variation, that is, more frequent occurrences and higher strength during equinoxes and rarer occurrences and weaker strength during solstices (e.g., Broun, 1848; Sabine, 1852). The semi-annual variations are reported in the occurrence rates and intensities of the magnetic storms (e.g., Cliver et al., 2000, 2004; Le Mouël et al., 2004; Cnossen and Richmond, 2012; Danilov et al., 2013; McPherron and Chu, 2018; Lockwood et al., 2020), and in the Earth's radiation belt electron variations (e.g., Baker et al., 1999; Li et al., 2001; Kanekal et al., 2010; Hajra, 2021a, and references therein). This is generally explained in the context of the Earth's position in the heliosphere (Cortie, 1912), relative angle of solar wind incidence with respect to Earth's rotation axis (Boller and Stolov, 1970), and geometrical controls of interplanetary magnetic fields (Russell and McPherron, 1973). See Lockwood et al. (2020) for an excellent discussion of the mechanisms.

However, the semi-annual variation in general was questioned by the work of Mursula et al. (2011) reporting solstice maxima in substorm frequency and duration, and substorm amplitude and global geomagnetic activity peaks alternating between spring and fall in ~ 11 years. While solstice maxima were attributed to auroral ionospheric conductivity changes (Wang and Lühr, 2007; Tanskanen et al., 2011), the alternating equinoctial maxima were associated to asymmetric solar wind distribution in solar hemispheres (Mursula and Zieger, 2001; Mursula et al., 2002).

In the present work, for the first time, we will explore a long-term database of HILDCAAs, substorms and magnetic storms of varying intensity along with different geomagnetic indices to study the seasonal features of geomagnetic disturbances. The main aims are to identify and characterize the seasonal features of geomagnetic disturbances of different types and intensities. In addition, we will study their solar activity dependencies, if any.

2 Database and Methods

Auroral substorms are identified by intensified auroral ionospheric (westward) electrojet currents. In the present work, we will use the substorm list available at the SuperMAG website (https://supermag.jhuapl.edu/, Newell and Gjerloev, 2011; Gjerloev, 2012). The substorm expansion phase onsets were identified from the SML index which is the SuperMAG equivalent of the westward auroral electrojet index AL (see the cited references for details). The present work involves a total of 75863 substorms identified from January 1976 to December 2019.

We will use the geomagnetic storm and HILDCAA database prepared by Hajra et al. (2021) for the present work. It is an updated version of the lists presented in Echer et al. (2011), Hajra et al. (2013), and Rawat et al. (2018). Geomagnetic storm onset, main phase, peak strength, recovery phase, and storm end are determined by the variations of the Dst index (Sugiura, 1964). Based on Gonzalez et al. (1994) definition, intervals with the Dst peak ≤ -50 nT are identified as magnetic storms. From January 1963 to December 2019, 1239 magnetic storms were identified. Geomagnetic storms with the Dst peak values between -50 nT and -100 nT are classified as moderate storms, between -100 nT and -250 nT as intense storms, and those with the Dst peaks lower than -250 nT as super storms.

https://doi.org/10.5194/angeo-2021-27
Preprint. Discussion started: 24 June 2021


Annales Geophysicae Discussions

The HILDCAA events are identified based on four criteria suggested by Tsurutani and Gonzalez (1987). They are: (1) the AE index should reach an intensity equal to or greater than 1000 nT at some point during the event (high-intensity criterion), (2) the event must last at least 2 days (long-duration criterion), (3) the AE index should not fall below 200 nT for more than 2 h at a time (continuity criterion), and (4) the auroral activity must occur outside of the main phase of geomagnetic storms or during non-storm conditions (Dst > -50 nT). Present work involves a total of 145 HILDCAA events identified during January 1975 through December 2017. It is important to note that from physical point of view, substorms and HILDCAAs are two different types of geomagnetic activity. While substorms occur during HILDCAAs, they represent different magnetosphere/ionosphere processes (Tsurutani et al., 2004; Guarnieri, 2005). Thus, for good reason, the term "substorm" was avoided in the definition of HILDCAAs by Tsurutani and Gonzalez (1987). Later, Hajra et al. (2014b, 2015a, b) have shown that HILDCAAs take important role in the acceleration of relativistic ($\sim$ MeV) electrons in the outer radiation belt of the Earth. This feature further distinguishes the HILDCAAs from nominal substorms. For further discussion on this topic (which is beyond the scope of the present work), we refer the interested reader to Tsurutani et al. (2004), and Guarnieri (2006).

The geomagnetic indices Dst, ap and AE are used to provide a quantitative measure of the activity level of the terrestrial magnetosphere (Rostoker, 1972). In addition to geomagnetic indices, solar wind parameters are important to study the energy dissipation in the magnetosphere. The D_{500} parameter corresponds to the percentage of days with the peak solar wind speed V_{sw} equal or higher than 500 km s^{-1}. This parameter indicates the occurrence of the solar wind high-speed streams (HSSs). We estimated the solar wind electric field VB_s, which is an important solar wind-magnetosphere coupling function. As VB_s involves both the solar wind velocity V_{sw} (for V) and the southward component of interplanetary magnetic field (IMF) B_s, the latter being important for magnetic reconnection, VB_s is also called the reconnection electric field. The Akasofu-ϵ coupling function (Perreault and Akasofu, 1978), obtained by $V_{sw}B_0^2 sin^4(\theta/2)R_{CF}^2$, was also estimated in this work as a proxy for the magnetospheric energy input rate. Here B_0 represents the magnitude of the IMF, θ is the IMF orientation clock angle, and R_{CF} corresponds to the Chapman-Ferraro magnetopause distance (Chapman and Ferraro, 1931).

We will apply Lomb-Scargle periodogram analysis (Lomb, 1976; Scargle, 1982) to identify dominant periodicities in the geomagnetic events, indices and solar wind-magnetosphere parameters. It is a useful tool for detecting and characterizing periodic signals for unequally spaced data.

The 10.7 cm solar flux ($F_{10.7}$) is shown to be a good indicator of the solar activity (e.g., Tapping, 1987). Thus, the $\sim$11-year solar cycles (Schwabe, 1844) are studied using the monthly mean $F_{10.7}$ solar flux variations. The starting, peak and end dates along with the peak $F_{10.7}$ flux of each solar cycle are listed in Table 1. The $F_{10.7}$ fluxes are given in the solar flux unit (sfu), where 1 sfu = 10^{-22} W m^{-2} Hz^{-1}. Based on the $F_{10.7}$ peaks, cycles SC20 and SC24 can be classified as the "weak cycles" (average $F_{10.7}$ peak $\sim$ 151 sfu), and SC19, SC21, SC22 and SC23 as the "strong cycles" (average $F_{10.7}$ peak $\sim$ 207 sfu). The solar cycles are also grouped into the "even" (SC20, SC22, SC24) and the "odd" (SC19, SC21, SC23) cycles in this work. It can be mentioned that SC24 is the weakest cycle in the space exploration era (after 1957). A detailed study on the solar and geomagnetic characteristics of this cycle is presented in Hajra (2021c).

https://doi.org/10.5194/angeo-2021-27
Preprint. Discussion started: 24 June 2021

Annales Geophysicae Discussions

Table 1. Details of the solar cycles under present study

SC no.	SC start date (year-month)	SC peak date (year-month)	SC peak $F_{10.7}$	SC end date (year-month)
SC20	1964-10	1968-11	156	1976-02
SC21	1976-03	1979-12	203	1986-08
SC22	1986-09	1989-11	213	1996-07
SC23	1996-08	2001-11	181	2008-11
SC24	2008-12	2014-04	146	2019-12

The geomagnetic indices are collected from the World Data Center for Geomagnetism, Kyoto, Japan (http://wdc.kugi.kyoto-u.ac.jp/). The monthly mean of solar wind/interplanetary data near the Earth's bow shock nose were obtained from NASA's OMNI database (http://omniweb.gsfc.nasa.gov/).

3 Results

3.1 Seasonal features

Figure 1 shows the variations of the monthly mean solar $F_{10.7}$ flux, HILDCAAs and substorms, magnetic storms of varying intensity, geomagnetic Dst, ap and AE indices, IMF magnitude B_0, solar wind plasma speed V_{sw}, percentage occurrences of $V_{sw} \geq 500$ km s^{-1} (D_{500}), and energy coupling functions VB_s and ϵ for the period from 1963 through 2019. Embedded in the large-scale ~ 11-year variations (most prominent in $F_{10.7}$), there are several short-term fluctuations in the data. Some of the latter may be associated with annual or semi-annual variations.

Monthly superposed variations

Figure 2 shows the monthly superposed values of all the parameters shown in Figure 1. The left panels show the numbers of geomagnetic events in each month normalized by the number of years of observations (in the unit of number per year). The right panels show the monthly means of the geomagnetic and solar wind/interplanetary parameters for the entire interval of study.

Substorm occurrence rate clearly exhibits two peaks during the months of March and October, and a summer solstice minimum (during the month of June). HILDCAAs do not exhibit any clear seasonal feature, except a significant minimum in November. Geomagnetic storms, from moderate to intense, exhibit a clear semi-annual variation. Spring equinoctial peak is recorded during March for moderate storms, and during April for intense storms, while the fall peak is recorded during October for both of them. Super storms, with a very low occurrence rate, do not have any clear seasonal feature. As majority of the storms are of moderate intensity, storms of all intensity together exhibit prominent semi-annual variation with two peaks during March and October.

https://doi.org/10.5194/angeo-2021-27
Preprint. Discussion started: 24 June 2021

Annales Geophysicae Discussions
Open Access
EGU

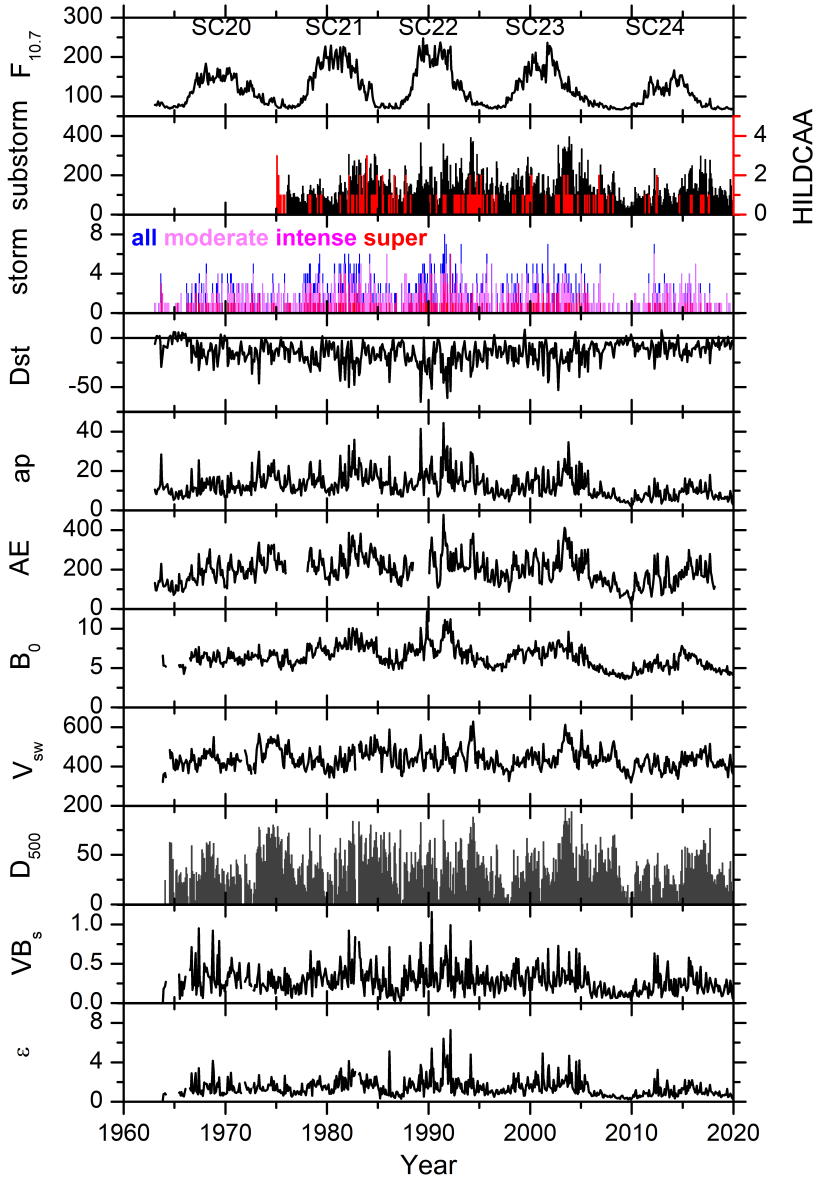

Figure 1. From top to bottom, the panels show the monthly mean solar $F_{10.7}$ flux (sfu), monthly numbers of substorms (black, legend on the left) and HILDCAAs (red, legend on the right) in the same panel, geomagnetic storms of varying intensity, monthly mean Dst (nT), ap (nT), AE (nT), IMF B_0 (nT), V_{sw} (km s^{-1}), percentage of days with daily peak $V_{sw} \geq 500$ km s^{-1} (D_{500}, %), VB_s (mV m^{-1}) and Akasofu ϵ-parameter (10^{11} W), respectively during 1963 through 2020. Solar cycles from SC20 through SC24 are marked on the top panel.

https://doi.org/10.5194/angeo-2021-27
Preprint. Discussion started: 24 June 2021

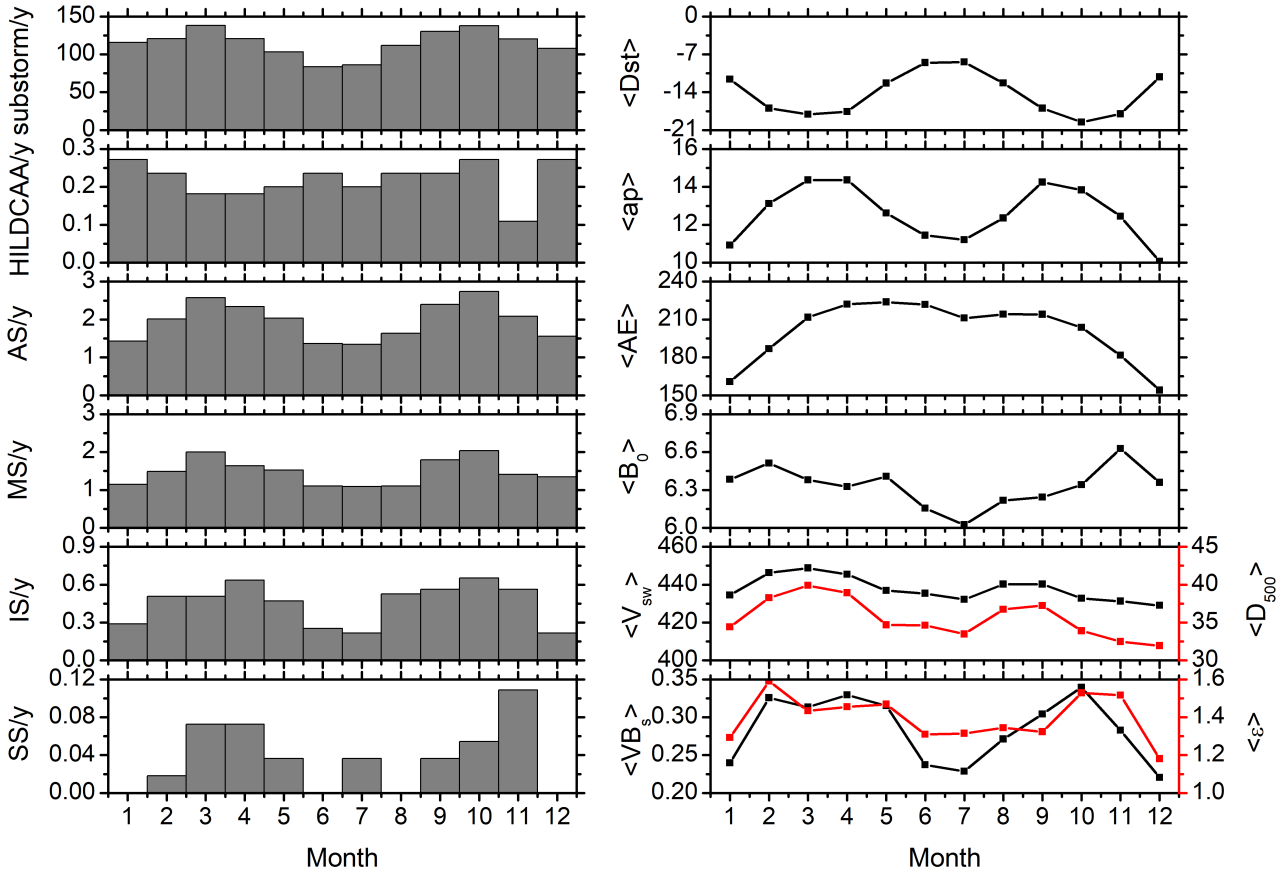

Figure 2. Monthly superposed variations. Left panels, from top to bottom, show the total numbers of substorms, HILDCAAs, all storms (AS), moderate (MS) and intense (IS) and super (SS) storms divided by numbers of the observing years, respectively. Right panels, from top to bottom, show the monthly mean values the geomagnetic Dst (nT), ap (nT) and AE (nT) indices, IMF B_0 (nT), V_{sw} (km s^{-1}, black, legend on the left), D_{500} (%, red, legend on the right) in the same panel, and VB_s (mV m^{-1}, black, legend on the left) and ϵ-parameter (10^{11} W, red, legend on the right) in the same panel, respectively.

https://doi.org/10.5194/angeo-2021-27
Preprint. Discussion started: 24 June 2021


Annales Geophysicae Discussions

The monthly mean intensities of the Dst and ap indices show a semi-annual variation. Both of them exhibit spring peaks during March. While Dst has a fall peak during October, ap exhibits a peak during September. On the other hand, the monthly mean AE index increases gradually from January, attains a peak around April, decreases with a much slower rate till September, after which the decrease rate is faster, and finally attains a minimum during December. Thus the AE index shows an annual variation, different from the Dst and ap indices. It is worth mentioning that the AE index (Davis and Sugiura, 1966) includes an upper envelope (AU) and a lower envelope (AL) related to the largest (positive) and smallest (negative) magnetic deflections, respectively among the magnetometer stations used. The AU and AL components are thought to represent the strengths of the eastward and westward AE, respectively. It is thus interesting to study the seasonal features of these components separately. This can be done in a future work.

Among the solar wind-magnetosphere coupling parameters, VB_s exhibits a semi-annual variation, with larger average values during February-April months, another sharp peak during October and with a solstice minimum. For the monthly mean IMF B_0, a clear minimum can be noted during July, and B_0 increases gradually on both sides of July. No clear seasonal features can be inferred from the variations of the monthly mean V_{sw}, D_{500} and Akasofu ϵ-parameter.

Periodogram analysis

It should be noted that the seasonal features as described above (Figure 2) present an average scenario composed by superposition of several solar cycles. This seasonal behaviour may have different behaviour in different solar cycles. In Figure 3 we have performed Lomb-Scargle periodogram analysis (Lomb, 1976; Scargle, 1982) of the above events and parameters.

As expected, the $F_{10.7}$ solar flux shows a prominent (at $> 95\%$ significance level) ~ 11-year periodicity (Figure 3, top panel). The same can be observed in substorms, HILDCAAs (Figure 3, second panel from the top), magnetic storms of varying intensity (Figure 3, third panel from the top), geomagnetic indices Dst, ap and AE (Figure 3, fourth panel from the top), and in solar wind/interplanetary parameters and solar wind-magnetosphere coupling functions B_0, V_{sw}, D_{500}, VB_s and ϵ (Figure 3, bottom panel). However, we are interested in annual or shorter-scale periodicities in the events and parameters.

Table 2 lists significant periodicities which are less than the ~ 11-year solar cycle period. As clear from Figure 3 and Table 2, substorms, moderate and intense geomagnetic storms exhibit prominent semi-annual (~ 6-month period) variation. However, super storms do not exhibit any clear variation pattern (not shown). HILDCAAs, on the other hand, exhibit a ~ 4.1-year periodicity, while no annual or lower-scale variation was recorded.

While the global-scale geomagnetic activity index ap and ring current index Dst exhibit a clear ~ 6-month periodicity, auroral ionospheric current related AE index exhibits an annual variation, but no semi-annual variation.

Solar wind/interplanetary and coupling functions exhibit more complex periodicity (lower than ~ 11-year). IMF B_0 and ϵ-parameter exhibit ~ 8-year periodicity, but no annual or lower-scale periodicity. Solar wind V_{sw} and D_{500} exhibit several periodicities in the range of $\sim 4-8$ years and a significant annual variation (periodicity ~ 1 year). The coupling function VB_s exhibits a prominent semi-annual variation. The V_{sw} periodicities detected in the present work are consistent with results reported previously (e.g., Valdés-Galicia et al., 1996; El-Borie, 2002; El-Borie et al., 2020; Hajra, 2021a; Hajra et al., 2021, and references therein). For example, El-Borie (2002) reported ~ 9.6-year periodicity in V_{sw} arising from the coronal hole

https://doi.org/10.5194/angeo-2021-27
Preprint. Discussion started: 24 June 2021

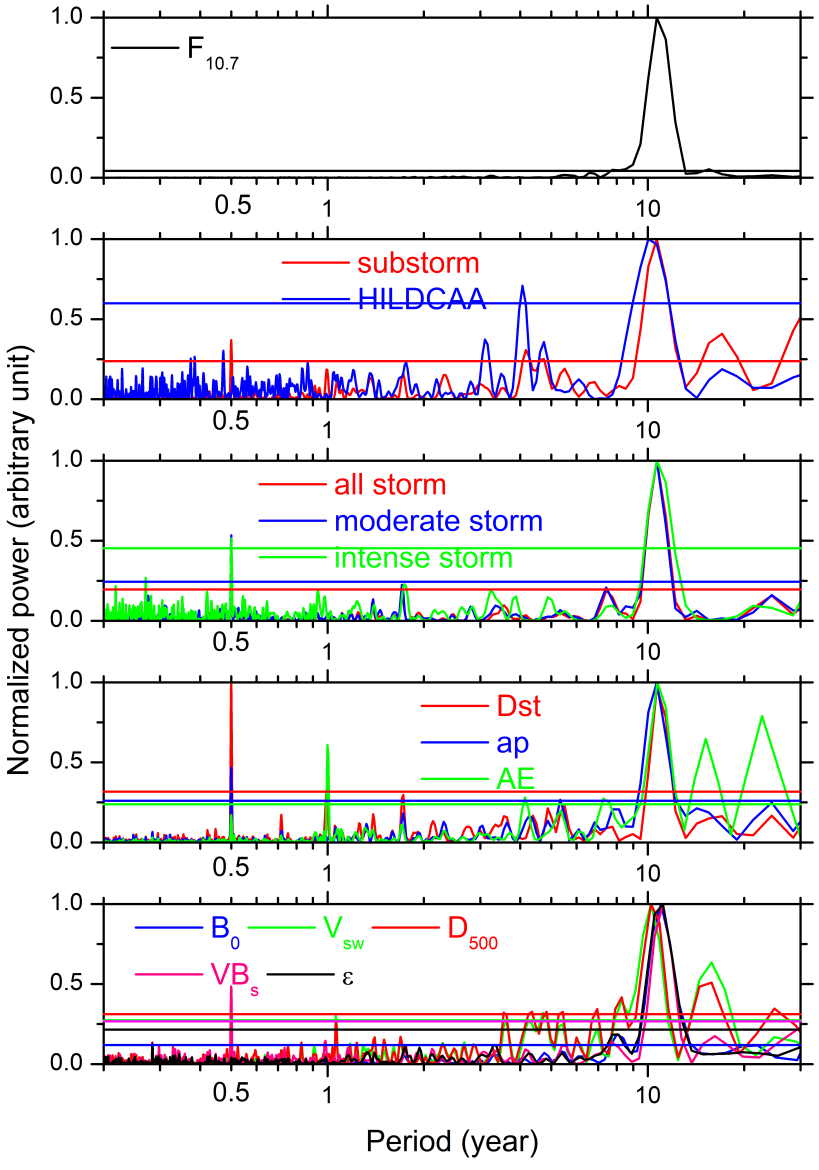

Figure 3. Lomb-Scargle periodograms. From top to bottom, the panels show the normalized power (arbitrary units) of periods (year) for the monthly mean solar $F_{10.7}$ flux, monthly occurrence rates of substorms and HILDCAAs in the same panel, all magnetic storms, moderate and intense storms in the same panel, geomagnetic indices Dst, ap and AE in the same panel, and solar wind parameters IMF B_0, V_{sw}, D_{500}, VB_s and ϵ-parameter in the same panel, respectively. Horizontal lines in each panel indicate $> 95\%$ significance levels of the corresponding parameters shown by different colors.

https://doi.org/10.5194/angeo-2021-27
Preprint. Discussion started: 24 June 2021

Annales Geophysicae Discussions

Table 2. Significant (at the $> 95\%$ level) periods less than ~ 11 years obtained from the Lomb-Scargle periodogram analysis. Periods are ordered from higher power to lower.

Events/parameters	Period (year)
geomagnetic activity:	
substorms	0.5, 4.2
HILDCAAs	4.1
all storms	0.5
moderate storms	0.5
intense storms	0.5
super storms	No
geomagnetic indices:	
Dst	0.5
ap	0.5
AE	1.0
solar wind parameters:	
B_0	8.0
V_{sw}	8.3, 4.7, 1.1
D_{500}	8.3, 7.0, 5.4, 4.8, 4.3, 3.6, 1.1
VB_s	0.5
ϵ	8.1

variations in the suthern hemisphere of the Sun. El-Borie et al. (2020) discussed multiple V_{sw} periodicities in the $1-2$-, $2-4$-, $4-8$- and $8-16$-year bands. Recently, Hajra et al. (2021) reported significant V_{sw} periodicities of ~ 3, ~ 4, ~ 10 and ~ 16 years and discussed their important role in space climatology.

The results shown in Figure 3 and Table 2 are consistent with those in Figure 2. From the above analyses, the coupling function VB_s which exhibits a ~ 6-month periodicity can be inferred as the driver of the semi-annual variations in substorms, moderate and intense storms, and in the geomagnetic indices Dst and ap. On the other hand, the ~ 1-year periodicity in V_{sw}/D_{500} can be a source of the annual variation in the AE index. Detailed analyses of the events and/or parameters which exhibit the annual and/or semi-annual variations are shown in Section 3.2. For a detailed analysis of the longer-scale variations of the geomagnetic activity, indices and solar wind-magnetosphere coupling, which is beyond the scope of this present work, we refer the read to Hajra et al. (2021).

3.2 Solar activity dependence

The solar cycle variations of the seasonal features described in Section 3.1 are explored in Figures 4 to 11. They show the variations of the substorms (Figure 4), moderate (Figure 5) and intense (Figure 6) magnetic storms, geomagnetic Dst (Figure 7),

https://doi.org/10.5194/angeo-2021-27
Preprint. Discussion started: 24 June 2021

Annales Geophysicae Discussions

Table 3. Seasonal modulation (%) between the equinoctial maximum and the solstice minimum for the events and the parameters with the semi-annual variation during the weak and strong solar cycles.

Events/parameters	Weak solar cycle	Strong solar cycle
substorms	55	46
all storms	85	76
moderate storms	92	73
intense storms	92	100
Dst	67	85
ap	40	37
VB_s	54	57

ap (Figure 8) and AE (Figure 9) indices, solar wind plasma speed V_{sw} (Figure 10), and coupling function VB_s (Figure 11). The format is the same: for the geomagnetic events (the solar wind interplanetary parameters), the bottom left panel shows the year-month contour plot of number of the events (the mean values) in each month of the observing years. The values of different colours are given in the legend at the bottom. The bottom right panel shows the yearly mean $F_{10.7}$ solar flux. The solar minima are marked by the horizontal dash-dot lines in the bottom panels. The second panel from the top shows the monthly numbers of the events per year of observation (monthly mean values of the parameters) during each solar cycles, while the top panel shows the same during groups of the even, odd, strong, weak and all solar cycles. Table 3 lists a seasonal modulation parameter defined as the difference between the equinoctial maximum and the solstice minimum expressed as the percentage of the yearly mean value for the events and parameters with semi-annual variation during the weak and strong solar cycles. The parameter can be taken as a measure of the seasonal/semi-annual variability. Larger the value of the parameter, stronger the semi-annual variability. They show almost similar variability between the weak and strong cycles.

Substorms

From Figure 4 (bottom left panel) it can be seen that in any solar cycle, the peak substorm occurrence rates are noted during the descending phase, followed by the occurrence minimum during the solar minimum to early ascending phase. From the complete 4 solar cycles (SCs 21–24) of the substorm observations, two prominent peaks can be noted in the years of 1994 and 2003, which are in the descending phases of the solar cycles 22 and 23, respectively.

On the seasonal basis, two peaks around the months of March and October can be observed from the year-month contour plot (Figure 4, bottom left panel), which is also reflected in the monthly superposed plots (top two panels). However, this "semi-annual" variation exhibits large asymmetry in amplitude and duration between the spring and fall equinoxes. For example, in the year 1994, the substorm occurrence peak during February-May is significantly larger than the occurrences during October. On the other hand, during 2003, while the occurrence peak is noted in November, comparable occurrences are clear almost during the entire year.

https://doi.org/10.5194/angeo-2021-27
Preprint. Discussion started: 24 June 2021

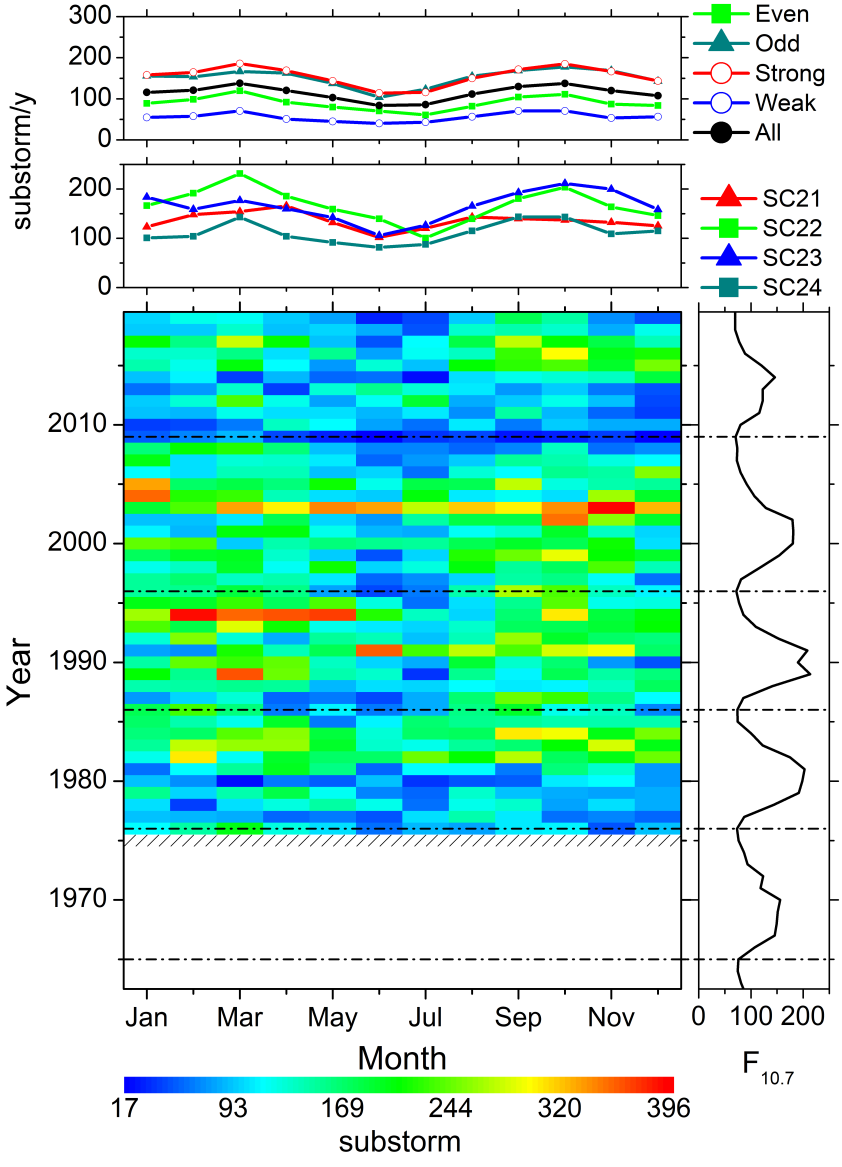

Figure 4. Substorms from 1976 through 2019. The bottom left panel shows the year-month contour plot of the number of substorms in each month of the years 1976-2019. The values of different colours are given in the legend at the bottom. Data gaps are shown by crosses. The bottom right panel shows the yearly mean $F_{10.7}$ solar flux (sfu). Second panel from the top shows the monthly numbers of substorms per a year of observation during each solar cycles, while the top panel shows the same during groups of the even, odd, strong, weak and all solar cycles. For details on the grouping of the solar cycles, see the text. The solar minima are marked by horizontal dash-dot lines.

https://doi.org/10.5194/angeo-2021-27
Preprint. Discussion started: 24 June 2021


Annales Geophysicae Discussions

When separated on the basis of solar cycles (Figure 4, top two panels), the smallest numbers of events are observed during SC24. Interestingly, the spring occurrences are the strongest in SC22 and the fall occurrences are the strongest in SC23. Another noteworthy feature is that the occurrence rates during the even and weak solar cycles are lower than during the odd and strong cycles, respectively. However, the seasonal modulation between the equinoctial maximum and the solstice minimum is comparable between the weak ($\sim 55\%$) and strong ($\sim 46\%$) cycles (Table 3).

Geomagnetic storms

Variations of the moderate and intense geomagnetic storms are shown in Figures 5 and 6, respectively. From the year-month contour plots, the moderate storms are found to peak around the descending phases, while the intense storms peak around the solar maximum. When monthly variations of the storms are considered in each year, there is hardly any seasonal variation. However, when observations during several solar cycles are grouped together, the semi-annual variations can be noted in the moderate storms. There is not much difference in moderate and intense storm occurrence rates between the odd and even cycles. However, the occurrence rates of the storms are slightly larger in the strong cycles compared to the weak ones, while seasonal modulation between the equinoctial maximum and the solstice minimum between the two is comparable (Table 3). Another noteworthy feature is the lowest occurrence of intense storms during the solar cycle 24 which is the weakest in space exploration era.

Geomagnetic indices

The variations of the monthly mean geomagnetic indices are shown in Figures 7 (Dst), 8 (ap) and 9 (AE). In each solar cycle, the average Dst index exhibits the strongest negative excursions at and immediately after the solar maximum (Figure 7). A clear correlation can be observed between the $F_{10.7}$ solar flux and the average Dst strength. The Dst negative excursions are stronger during the strong and odd cycles compared to the weak and even cycles, respectively. In addition, the seasonal modulation between the equinox minimum to the solstice maximum is significantly higher in the strong cycles ($\sim 85\%$) compared to the weak cycles ($\sim 67\%$) (Table 3). During SC24, the overall Dst strength is the weakest and there is no prominent seasonal modulation.

The variation of the monthly mean ap index (Figure 8) is identical to the Dst index variation. However, the seasonal modulation is comparable between the strong ($\sim 37\%$) and weak ($\sim 40\%$) cycles for the ap index (Table 3).

The variation of the AE index (Figure 9) is significantly different than the variations of the Dst and ap indices. In a solar cycle, AE peaks around the descending phase. On the yearly basis, the average AE values are enhanced from March/April to September/October. The summer solstice values are significantly higher compared to the winter solstice values. This indicates an annual variation, in agreement with the Lomb-Scargle periodogram (Figure 3). There is no semi-annual variation. The average values during the strong and odd solar cycles are higher compared to the weak and even solar cycles, respectively. SC24 exhibited the lowest values of AE compared to other solar cycles.

https://doi.org/10.5194/angeo-2021-27
Preprint. Discussion started: 24 June 2021

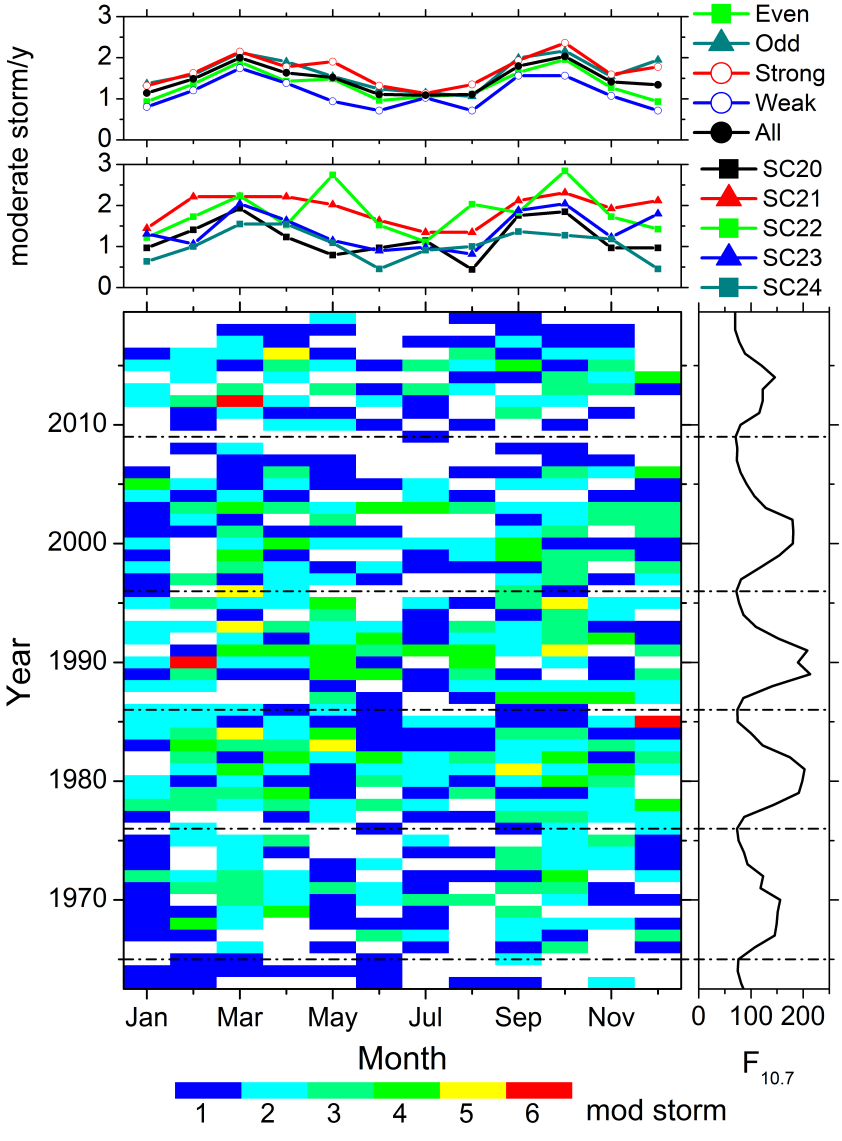

Figure 5. Moderate geomagnetic storms from 1963 through 2019. The panels are in the same format as in Figure 4.

https://doi.org/10.5194/angeo-2021-27
Preprint. Discussion started: 24 June 2021

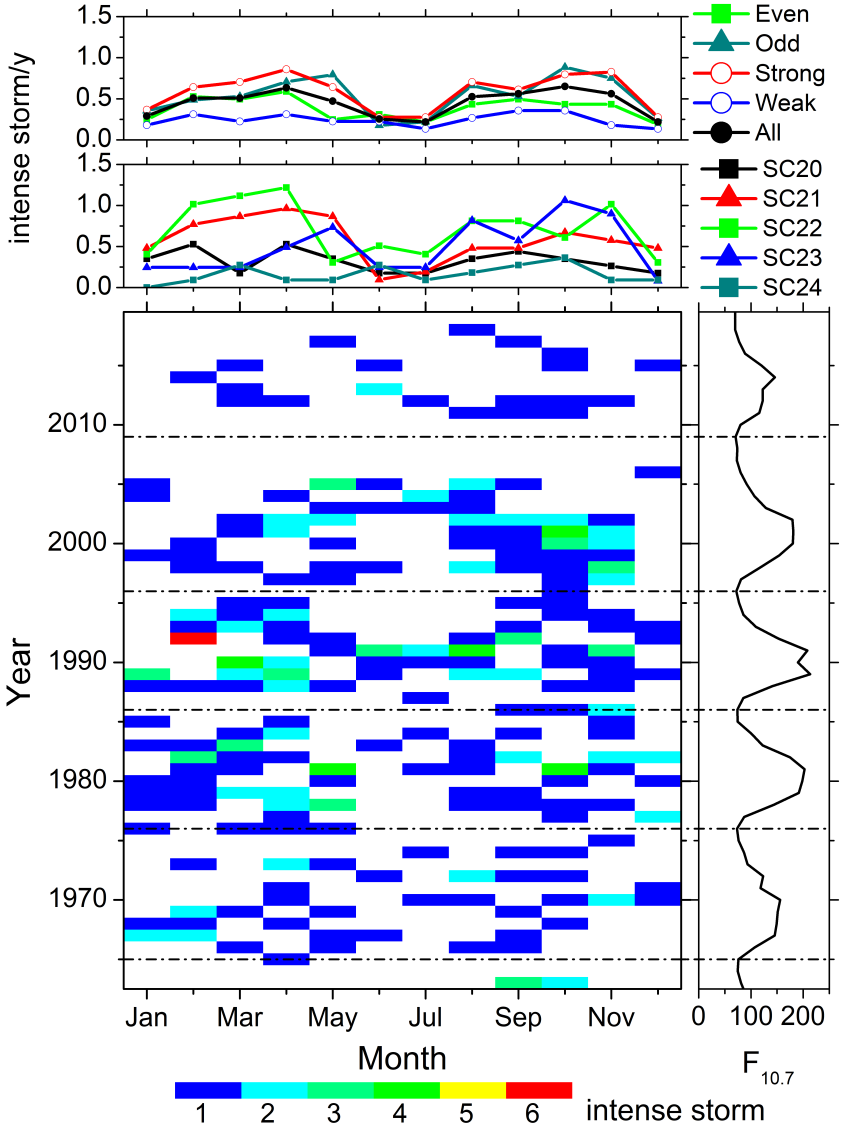

Figure 6. Intense geomagnetic storms from 1963 through 2019. The panels are in the same format as in Figure 4.

https://doi.org/10.5194/angeo-2021-27
Preprint. Discussion started: 24 June 2021

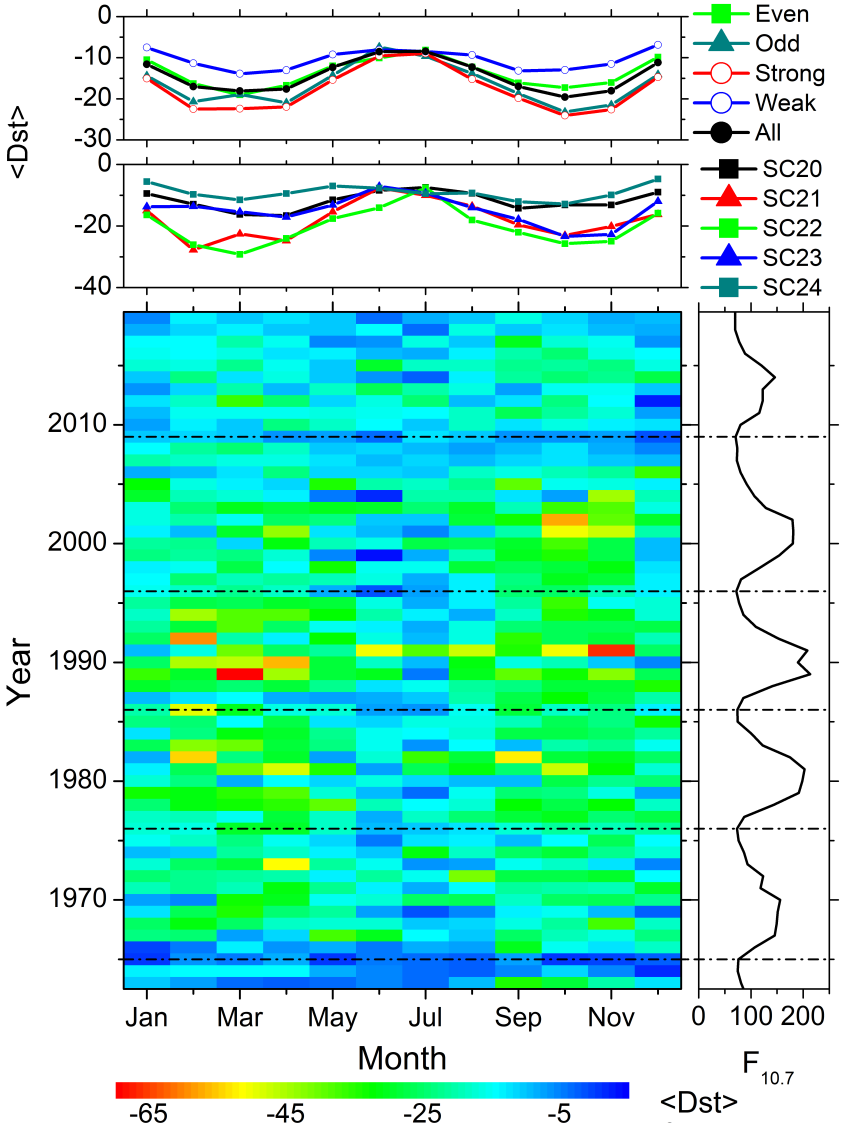

Figure 7. Geomagnetic Dst index (nT) variation from 1963 through 2019. The bottom left panel shows the year-month contour plot of the mean Dst value (nT) in each month of the years 1963-2019. The values of different colours are given in the legend at the bottom. Data gaps are shown by crosses. The bottom right panel shows the yearly mean F10.7 solar flux (sfu). Second panel from the top shows the monthly means of Dst (nT) during each solar cycles, while the top panel shows the same during groups of the even, odd, strong, weak and all solar cycles.

https://doi.org/10.5194/angeo-2021-27
Preprint. Discussion started: 24 June 2021

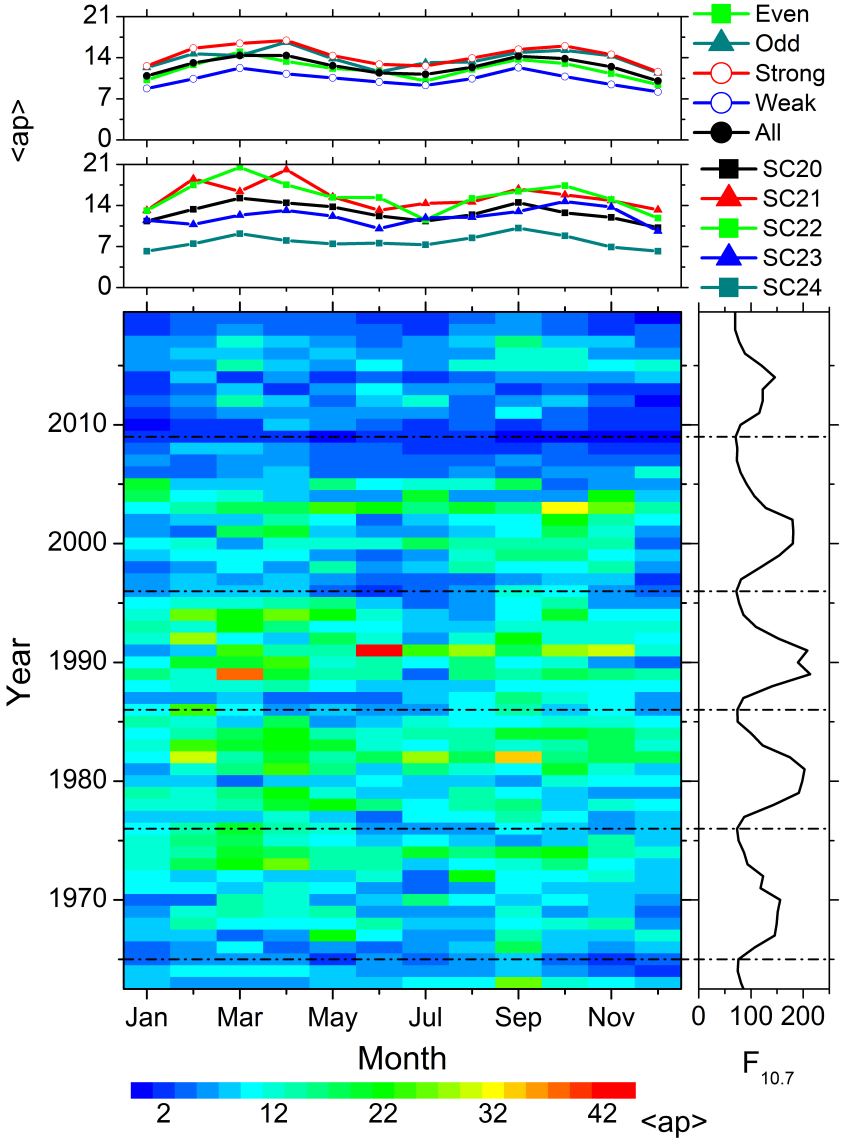

Figure 8. Geomagnetic ap index (nT) variation from 1963 through 2019. The panels are in the same format as in Figure 7.

https://doi.org/10.5194/angeo-2021-27
Preprint. Discussion started: 24 June 2021

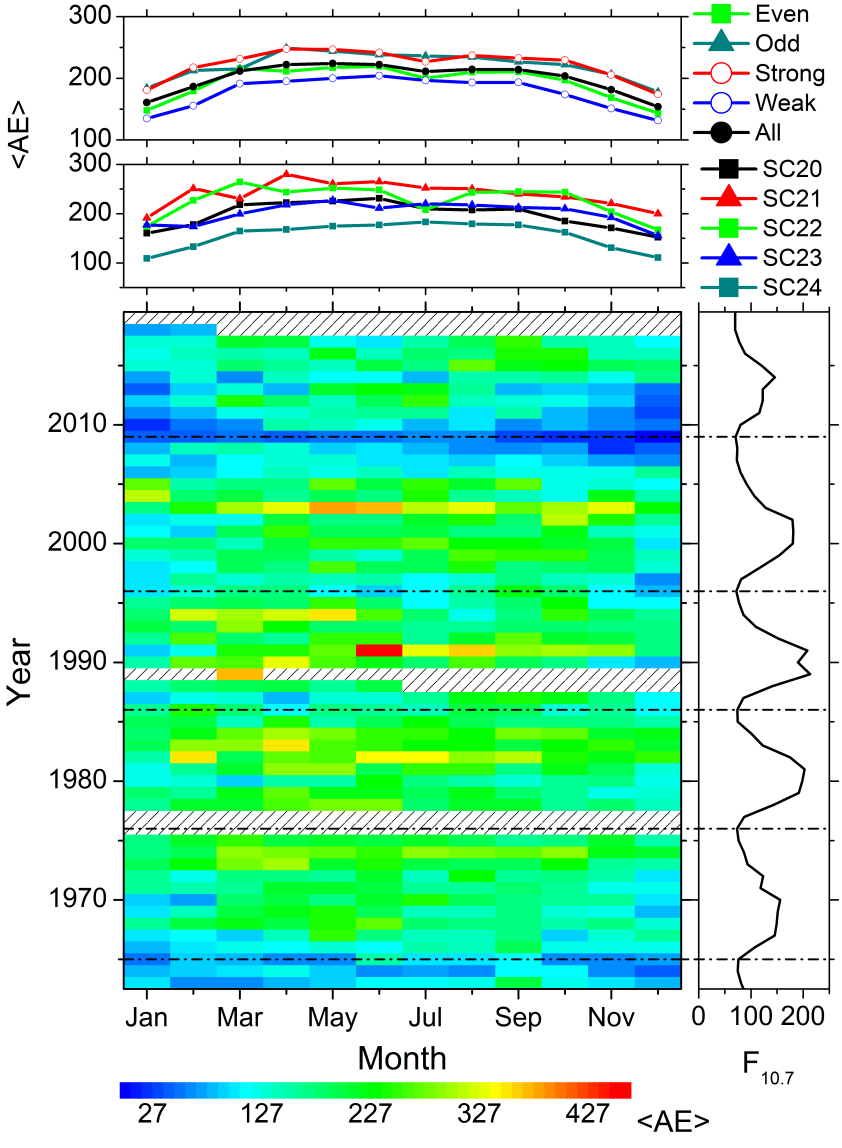

Figure 9. Geomagnetic AE index (nT) variation from 1963 through 2019. The panels are in the same format as in Figure 7.

https://doi.org/10.5194/angeo-2021-27
Preprint. Discussion started: 24 June 2021

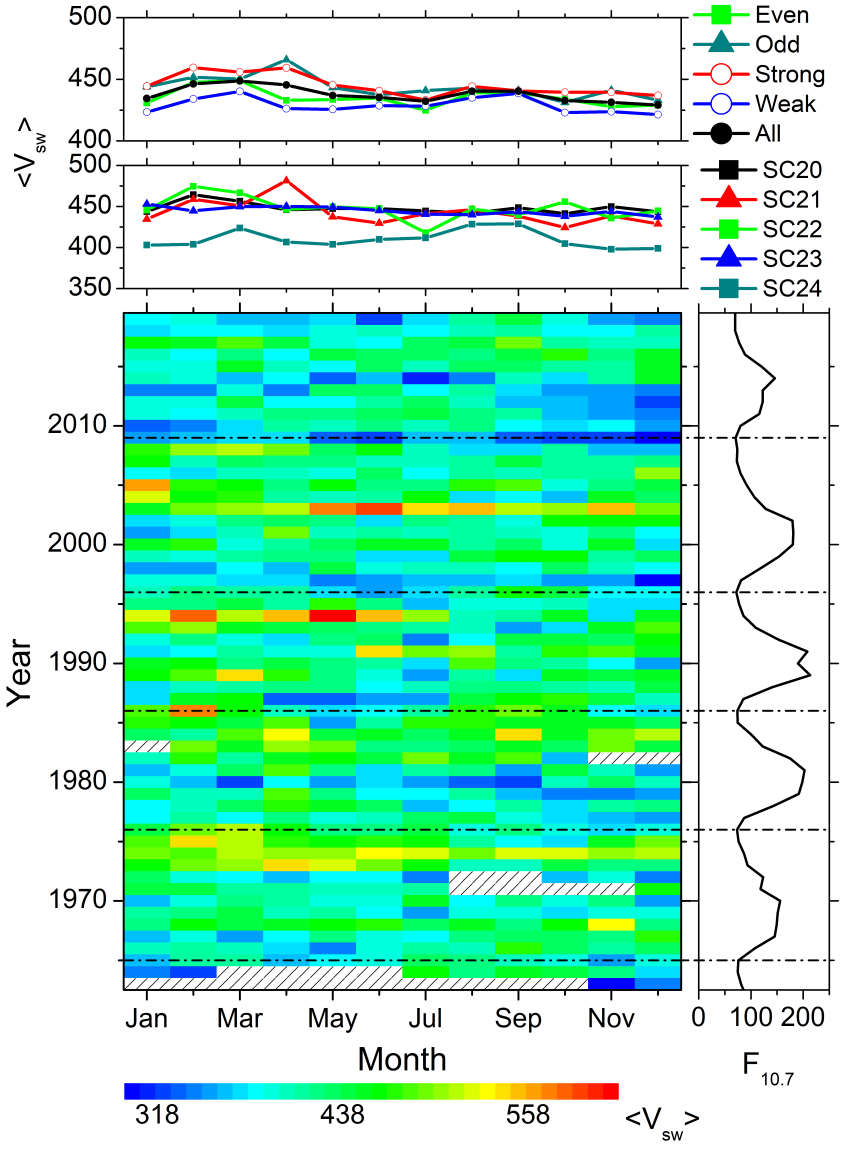

Figure 10. Solar wind speed V_{sw} (km s^{-1}) variation from 1963 through 2019. The panels are in the same format as in Figure 7.

Solar wind-magnetosphere coupling

The periodogram analysis (Figure 3 and Table 2) identified a weak annual component in the variations of the solar wind speed V_{sw} (compared with its stronger amplitude longer-scale variations). The monthly means values of V_{sw} during each year of observation are shown in Figure 10 (bottom left panel). In a solar cycle, V_{sw} peaks around the descending phase indicating a

https://doi.org/10.5194/angeo-2021-27
Preprint. Discussion started: 24 June 2021


Annales Geophysicae Discussions

higher occurrence rate of the HSSs during this phase. This is also confirmed by the variations of D_{500} (not shown). Interestingly, during the descending phase of SC20, the V_{sw} peak can be noted around March-April; during the SC21 descending phase, two equinoctial peaks are almost symmetric; during the SC22 descending phase peaks are recorded during the first half of the year; they shift to the second half of the year during the SC23 descending phase; and during the SC24 descending phase, no prominent feature can be inferred. Thus, overall, a shift of the seasonal peak of V_{sw} from the first half to the second half of the year can be observed between the even and the odd cycles. In addition, during the first half of the year, the average values are significantly high during the odd and strong cycles than during the even and weak cycles, respectively.

Figure 11 shows the monthly means values of the coupling function VB_s during all years of observation. In a solar cycle, VB_s peaks around the solar maximum, when almost symmetrical peaks can be observed during the equinoxes and minima during the solstices. The lowest values of VB_s are recorded during SC24. There is no prominent difference between the weak and strong cycles, and between the even and odd cycles, except that the February and October values are higher during odd and strong cycles compared to those during the even and the weak cycles, respectively.

4 Conclusions

We used an up-to-date list of substorms, HILDCAAs and geomagnetic storms of varying intensity along with all available geomagnetic indices during the space exploration era (i.e., after 1957) to explore the seasonal features of the geomagnetic activity and their drivers. No such study involving such a long database and all types of geomagnetic activity has been reported before. As substorms, HILDCAAs and magnetic storms of varying intensity have varying solar/interplanetary drivers, such a study is important for a complete understanding of the seasonal features of the geomagnetic response to the solar/interplanetary events. The main findings of this work are discussed below.

Firstly, the semi-annual variation is not a "universal" feature of the geomagnetic activity. While substorms, moderate and intense magnetic storms exhibit the semi-annual variation with two equinoctial maxima and a summer solstice minimum, super storms (with very low occurrence rate) and HILDCAA events do not exhibit any clear seasonal dependence. For geomagnetic indices, the ring current index Dst and the global geomagnetic activity index ap exhibit the semi-annual variation, while the auroral ionospheric electrojet current index AE exhibits an annual variation with a summer solstice maximum and a winter minimum. These results clearly demonstrate varying solar, interplanetary, magnetospheric and ionospheric processes behind the geomagnetic events and indices. While the magnetic reconnection (Dungey, 1961) between the southward IMF and the northward dayside geomagnetic field is the key for any geomagnetic effect, variation in the reconnection process and modulation by other processes may result in different geomagnetic effects (e.g., Gonzalez et al., 1994; Hajra, 2021a; Hajra et al., 2021, and references therein). In general, major magnetic storms are associated with strong magnetic reconnection continuing for a few hours, weaker reconnection for an hour or less can cause substorms. On the other hand, discrete and weaker magnetic reconnection continuing for a long interval of time may lead to HILDCAAs.

The results obtained in the present work reveal a clear semi-annual component in the coupling function VB_s which represents the reconnection electric field or the magnetic flux transfer rate into the magnetosphere. On the other hand, the solar

https://doi.org/10.5194/angeo-2021-27
Preprint. Discussion started: 24 June 2021

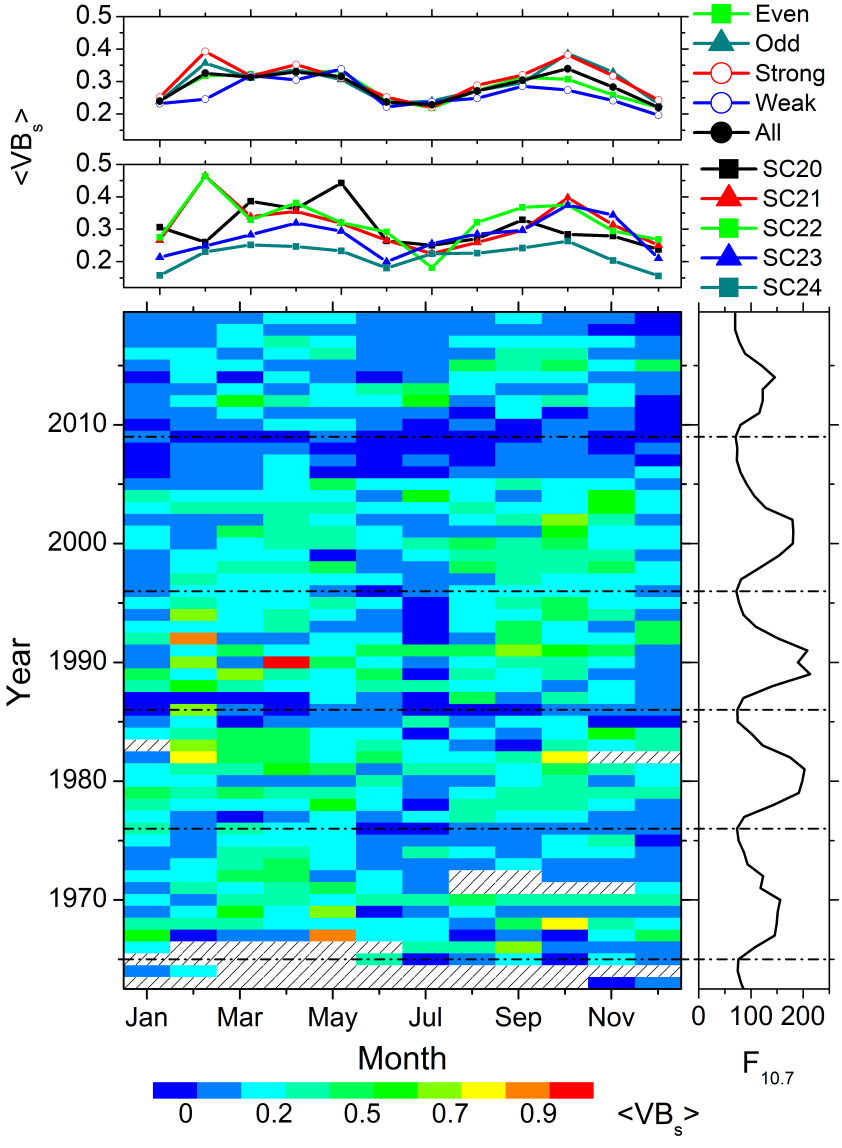

Figure 11. Solar wind coupling function VB_s (mV m^{-1}) variation from 1963 through 2019. The panels are in the same format as in Figure 7.

https://doi.org/10.5194/angeo-2021-27
Preprint. Discussion started: 24 June 2021


Annales Geophysicae Discussions

wind speed V_{sw} does not have any semi-annual component, only annual and longer-scale components. As the main focus of the present work is the seasonal features, for a discussion on the longer-scale variations in V_{sw}, we refer the reader to previous works (e.g., Valdés-Galicia et al., 1996; El-Borie, 2002; El-Borie et al., 2020; Hajra, 2021a; Hajra et al., 2021, and references therein). However, this result is very interesting. This clearly implies that the solar wind does not have any intrinsic semi-annual variation, and that the semi-annual variation in VB_s is due to magnetic configuration (B_s) as suggested previously (e.g., Cortie, 1912; McIntosh, 1959; Boller and Stolov, 1970; Russell and McPherron, 1973). This has a large contribution in the semi-annual variations of the substorms, moderate and intense storms, and geomagnetic Dst and ap indices. On the other hand, absence of any clear seasonal features in super storms and HILDCAAs indicates more complex solar wind-magnetic coupling process during these events, which needs further study. As previously established, HILDCAAs are associated with HSSs emanated from the solar coronal holes (e.g., Tsurutani and Gonzalez, 1987; Hajra et al., 2013). Dominating longer-scale variations in V_{sw} (as revealed in the present work) may be a plausible reason for lack of any seasonal feature in HILDCAAs (Hajra et al., 2014a; Hajra, 2021c). Annual variation in the auroral ionospheric AE index may be attributed to the ionospheric conductivity variations (see, e.g., Wang and Lühr, 2007; Tanskanen et al., 2011).

In addition to the above, we found a clear solar activity dependence of the above-mentioned seasonal features. The spring-fall asymmetry in substorms and average V_{sw} variation between odd and even solar cycles are consistent with results reported by Mursula et al. (2011). While semi-annual variability (seasonal modulation between the equinoctial maximum and the solstice minimum) was comparable between the strong and weak solar cycles, the overall occurrence rate of the geomagnetic events and the average values of the parameters were significantly stronger during the odd and strong cycles compared to the even and weak cycles, respectively. Further study is required for a better understanding of the solar cycle dependencies of the geomagnetic activity seasonal features. In conclusion, this study, along with several previous works (e.g., Mursula et al., 2011; Hajra et al., 2013, 2016; Hajra, 2021a), calls for the careful re-analyses of the solar, interplanetary, magnetospheric and ionospheric observations before applying theoretical semi-annual models.

Data availability. The solar wind plasma and IMF data used in this work are obtained from the OMNI website (https://omniweb.gsfc.nasa.gov/). The geomagnetic indices are obtained from the World Data Center for Geomagnetism, Kyoto, Japan (http://wdc.kugi.kyoto-u.ac.jp/). The list of substorms is collected from the SuperMAG website (https://supermag.jhuapl.edu/).

Author contributions. RH had the original idea. AMSF and RH did the data analysis. RH prepared the first draft. All authors participated in the development of the manuscript and approved the final draft.

Competing interests. Authors declare that there is no competing interest.

https://doi.org/10.5194/angeo-2021-27
Preprint. Discussion started: 24 June 2021

Annales Geophysicae Discussions
Open Access
EGU

Acknowledgements. The work of A. M. S. F. is funded by the Brazilian CNPq agency (project no. PQ-300969/2020-1, PQ-301542/2021-0). The work of R. H. is funded by the Science and Engineering Research Board (SERB, grant no. SB/S2/RJN-080/2018), a statutory body of the Department of Science and Technology (DST), Government of India through Ramanujan fellowship. E. E. would like to thank Brazilian agencies for research grants: CNPq (contract no. PQ-302583/2015-7, PQ-301883/2019-0) and FAPESP (2018/21657-1). The work of M. J. A. B. was supported by CNPq agency (contract no. PQ-302330/2015-1, PQ-305692/2018-6) and FAPEG agency (contract no. 2012.1026.7000905).

https://doi.org/10.5194/angeo-2021-27
Preprint. Discussion started: 24 June 2021

References

Akasofu, S.-I.: The development of the auroral substorm, Planet. Space Sci., 12, 273–282, https://doi.org/10.1016/0032-0633(64)90151-5, 1964.

Axford, W. I. and Hines, C. O.: A UNIFYING THEORY OF HIGH-LATITUDE GEOPHYSICAL PHENOMENA AND GEOMAGNETIC STORMS, Can. J. Phys., 39, 1433–1464, https://doi.org/10.1139/p61-172, 1961.

Baker, D. N., Kanekal, S. G., Pulkkinen, T. I., and Blake, J. B.: Equinoctial and solstitial averages of magnetospheric relativistic electrons: A strong semiannual modulation, Geophys. Res. Lett., 26, 3193–3196, https://doi.org/10.1029/1999GL003638, 1999.

Boller, B. R. and Stolov, H. L.: Kelvin-Helmholtz instability and the semiannual variation of geomagnetic activity, J. Geophys. Res., 75, 6073–6084, https://doi.org/10.1029/JA075i031p06073, 1970.

Broun, J. A.: Observations in magnetism and meteorology made at Makerstoun in Scotland, Trans. R. Soc. Edinburgh., 18, 401–402, 1848.

Chapman, S. and Ferraro, V. C. A.: A new theory of magnetic storms, Terr. Mag. Atmos. Elec., 36, 77–97, https://doi.org/10.1029/TE036i002p00077, 1931.

Cliver, E. W., Kamide, Y., and Ling, A. G.: Mountains versus valleys: Semiannual variation of geomagnetic activity, J. Geophys. Res. Space Phys., 105, 2413–2424, https://doi.org/10.1029/1999JA900439, 2000.

Cliver, E. W., Svalgaard, L., and Ling, A. G.: Origins of the semiannual variation of geomagnetic activity in 1954 and 1996, Ann. Geophys., 22, 93–100, https://doi.org/10.5194/angeo-22-93-2004, 2004.

Cnossen, I. and Richmond, A. D.: How changes in the tilt angle of the geomagnetic dipole affect the coupled magnetosphere-ionosphere-thermosphere system, J. Geophys. Res. Space Phys., 117, https://doi.org/10.1029/2012JA018056, 2012.

Cortie, A. L., S.: Sun-spots and Terrestrial Magnetic Phenomena, 1898–1911: the Cause of the Annual Variation in Magnetic Disturbances, Mon. Not. Roy. Astron. Soc., 73, 52–60, https://doi.org/10.1093/mnras/73.1.52, 1912.

Danilov, A. A., Krymskii, G. F., and Makarov, G. A.: Geomagnetic activity as a reflection of processes in the magnetospheric tail: 1. The source of diurnal and semiannual variations in geomagnetic activity, Geomag. Aeron., 53, 469–475, https://doi.org/10.1134/S0016793213040051, 2013.

Davis, T. N. and Sugiura, M.: Auroral electrojet activity index AE and its universal time variations, J. Geophys. Res., 71, 785–801, https://doi.org/10.1029/JZ071i003p00785, 1966.

Dungey, J. W.: Interplanetary Magnetic Field and the Auroral Zones, Phys. Rev. Lett., 6, 47–48, https://doi.org/10.1103/PhysRevLett.6.47, 1961.

Echer, E., Gonzalez, W. D., and Tsurutani, B. T.: Statistical studies of geomagnetic storms with peak Dst $\leq$ -50 nT from 1957 to 2008, J. Atmos. Sol. Terr. Phys., 73, 1454–1459, https://doi.org/10.1016/j.jastp.2011.04.021, 2011.

El-Borie, M.: On Long-Term Periodicities In The Solar-Wind Ion Density and Speed Measurements During The Period 1973–2000, Sol. Phys., 208, 345–358, https://doi.org/10.1023/A:1020585822820, 2002.

El-Borie, M., El-Taher, A., Thabet, A., and Bishara, A.: The Interconnection between the Periodicities of Solar Wind Parameters Based on the Interplanetary Magnetic Field Polarity (1967–2018): A Cross Wavelet Analysis, Sol. Phys., 295, 122, https://doi.org/10.1007/s11207-020-01692-2, 2020.

Gjerloev, J. W.: The SuperMAG data processing technique, J. Geophys. Res., 117, https://doi.org/10.1029/2012JA017683, 2012.

Gonzalez, W. D., Joselyn, J. A., Kamide, Y., Kroehl, H. W., Rostoker, G., Tsurutani, B. T., and Vasyliunas, V. M.: What is a geomagnetic storm?, J. Geophys. Res., 99, 5771–5792, https://doi.org/10.1029/93JA02867, 1994.

https://doi.org/10.5194/angeo-2021-27
Preprint. Discussion started: 24 June 2021

Guarnieri, F. L.: TStudy of the solar and interplanetary origin of long-duration and continuous auroral activity events, Ph.D. thesis, INPE, http://livros01.livrosgratis.com.br/cp012558.pdf, 2005.

Guarnieri, F. L.: The nature of auroras during high-intensity long-duration continuous AE activity (HILDCAA) events: 1998 to 2001, pp. 235–243, American Geophysical Union (AGU), https://doi.org/10.1029/167GM19, 2006.

Hajra, R.: Seasonal dependence of the Earth's radiation belt – new insights, Ann. Geophys., 39, 181–187, https://doi.org/10.5194/angeo-39-181-2021, 2021a.

Hajra, R.: September 2017 Space-Weather Events: A Study on Magnetic Reconnection and Geoeffectiveness, Sol. Phys., 296, 50, https://doi.org/10.1007/s11207-021-01803-7, 2021b.

Hajra, R.: Weakest Solar Cycle of the Space Age: A Study on Solar Wind–Magnetosphere Energy Coupling and Geomagnetic Activity, Sol. Phys., 296, 33, https://doi.org/10.1007/s11207-021-01774-9, 2021c.

Hajra, R., Echer, E., Tsurutani, B. T., and Gonzalez, W. D.: Solar cycle dependence of High-Intensity Long-Duration Continuous AE Activity (HILDCAA) events, relativistic electron predictors?, J. Geophys. Res. Space Phys., 118, 5626–5638, https://doi.org/10.1002/jgra.50530, 2013.

Hajra, R., Echer, E., Tsurutani, B. T., and Gonzalez, W. D.: Superposed epoch analyses of HILDCAAs and their interplanetary drivers: Solar cycle and seasonal dependences, J. Atmos. Sol. Terr. Phys., 121, 24–31, https://doi.org/10.1016/j.jastp.2014.09.012, 2014a.

Hajra, R., Tsurutani, B. T., Echer, E., and Gonzalez, W. D.: Relativistic electron acceleration during high-intensity, long-duration, continuous AE activity (HILDCAA) events: Solar cycle phase dependences, Geophys. Res. Lett., 41, 1876–1881, https://doi.org/10.1002/2014GL059383, 2014b.

Hajra, R., Tsurutani, B. T., Echer, E., Gonzalez, W. D., Brum, C. G. M., Vieira, L. E. A., and Santolik, O.: Relativistic electron acceleration during HILDCAA events: are precursor CIR magnetic storms important?, Earth Planets Space, 67, 109, https://doi.org/10.1186/s40623-015-0280-5, 2015a.

Hajra, R., Tsurutani, B. T., Echer, E., Gonzalez, W. D., and Santolik, O.: Relativistic (E$>$ 0.6, $>$ 2.0, and $>$ 4.0 MeV) electron acceleration at geosynchronous orbit during high-intensity, long-duration, continuous AE activity (HILDCAA) events, Astrophys. J., 799, 39, https://doi.org/10.1088/0004-637x/799/1/39, 2015b.

Hajra, R., Tsurutani, B. T., Echer, E., Gonzalez, W. D., and Gjerloev, J. W.: Supersubstorms (SML $<$ -2500 nT): Magnetic storm and solar cycle dependences, J. Geophys. Res. Space Phys., 121, 7805–7816, https://doi.org/10.1002/2015JA021835, 2016.

Hajra, R., Franco, A. M. S., Echer, E., and Bolzan, M. J. A.: Long-term variations of the geomagnetic activity: a comparison between the strong and weak solar activity cycles and implications for the space climate, J. Geophys. Res. Space Phys., 126, e2020JA028 695, https://doi.org/10.1029/2020JA028695, 2021.

Kanekal, S. G., Baker, D. N., and McPherron, R. L.: On the seasonal dependence of relativistic electron fluxes, Ann. Geophys., 28, 1101–1106, https://doi.org/10.5194/angeo-28-1101-2010, 2010.

Lakhina, G. S. and Tsurutani, B. T.: Chapter 7 - Supergeomagnetic Storms: Past, Present, and Future, in: Extreme Events in Geospace: Origins, Predictability, and Consequences, edited by Buzulukova, N., pp. 157–185, Elsevier, https://doi.org/10.1016/B978-0-12-812700-1.00007-8, 2018.

Le Mouël, J.-L., Blanter, E., Chulliat, A., and Shnirman, M.: On the semiannual and annual variations of geomagnetic activity and components, Ann. Geophys., 22, 3583–3588, https://doi.org/10.5194/angeo-22-3583-2004, 2004.

Li, X., Baker, D. N., Kanekal, S. G., Looper, M., and Temerin, M.: Long term measurements of radiation belts by SAMPEX and their variations, Geophys. Res. Lett., 28, 3827–3830, https://doi.org/10.1029/2001GL013586, 2001.

https://doi.org/10.5194/angeo-2021-27
Preprint. Discussion started: 24 June 2021

Lockwood, M., Owens, M. J., Barnard, L. A., Haines, C., Scott, C. J., McWilliams, K. A., and Coxon, J. C.: Semi-annual, annual and Universal Time variations in the magnetosphere and in geomagnetic activity: 1. Geomagnetic data, J. Space Weath. Space Clim., 10, 23, https://doi.org/10.1051/swsc/2020023, 2020.

Lomb, N. R.: Least-squares frequency analysis of unequally spaced data, Astrophys. Space Sci., 39, 447–462, https://doi.org/10.1007/BF00648343, 1976.

McIntosh, D. H.: On the annual variation of magnetic disturbance, Philosophical Transactions of the Royal Society of London. Series A, Mathematical and Physical Sciences, 251, 525–552, https://doi.org/10.1098/rsta.1959.0010, 1959.

McPherron, R. L. and Chu, X.: The Midlatitude Positive Bay Index and the Statistics of Substorm Occurrence, J. Geophys. Res., 123, 2831–2850, https://doi.org/10.1002/2017JA024766, 2018.

Mursula, K. and Zieger, B.: Long-term north-south asymmetry in solar wind speed inferred from geomagnetic activity: A new type of century-scale solar oscillation?, Geophys. Res. Lett., 28, 95–98, https://doi.org/10.1029/2000GL011880, 2001.

Mursula, K., Hiltula, T., and Zieger, B.: Latitudinal gradients of solar wind speed around the ecliptic: Systematic displacement of the streamer belt, Geophys. Res. Lett., 29, 1–4, https://doi.org/10.1029/2002Gl015318, 2002.

Mursula, K., Tanskanen, E., and Love, J. J.: Spring-fall asymmetry of substorm strength, geomagnetic activity and solar wind: Implications for semiannual variation and solar hemispheric asymmetry, Geophys. Res. Lett., 38, https://doi.org/10.1029/2011GL046751, 2011.

Newell, P. T. and Gjerloev, J. W.: Evaluation of SuperMAG auroral electrojet indices as indicators of substorms and auroral power, J. Geophys. Res., 116, https://doi.org/10.1029/2011JA016779, 2011.

Perreault, P. and Akasofu, S.-I.: A study of geomagnetic storms, Geophys. J. Roy. Astron. Soc., 54, 547–573, https://doi.org/10.1111/j.1365-246X.1978.tb05494.x, 1978.

Rawat, R., Echer, E., and Gonzalez, W. D.: How Different Are the Solar Wind-Interplanetary Conditions and the Consequent Geomagnetic Activity During the Ascending and Early Descending Phases of the Solar Cycles 23 and 24?, J. Geophys. Res. Space Phys., 123, 6621–6638, https://doi.org/10.1029/2018JA025683, 2018.

Rostoker, G.: Geomagnetic indices, Rev. Geophys., 10, 935–950, https://doi.org/10.1029/RG010i004p00935, 1972.

Russell, C. T. and McPherron, R. L.: Semiannual variation of geomagnetic activity, J. Geophys. Res., 78, 92–108, https://doi.org/10.1029/JA078i001p00092, 1973.

Sabine, E.: VIII. On periodical laws discoverable in the mean effects of the larger magnetic disturbance. 2014;No. II, Phil. Tran. Roy. Soc. Lon., 142, 103–124, https://doi.org/10.1098/rstl.1852.0009, 1852.

Scargle, J. D.: Studies in astronomical time series analysis. II. Statistical aspects of spectral analysis of unevenly spaced data, Astrophys. J., 263, 835–853, 1982.

Schwabe, H.: Sonnen-Beobachtungen im Jahre 1843, Astron. Nach., 21, 233–236, 1844.

Sugiura, M.: Hourly values of equatorial Dst for the IGY, Ann. Intern. Geophys. Year, 35, 9, 1964.

Tanskanen, E. I., Pulkkinen, T. I., Viljanen, A., Mursula, K., Partamies, N., and Slavin, J. A.: From space weather toward space climate time scales: Substorm analysis from 1993 to 2008, J. Geophys. Res., 116, https://doi.org/10.1029/2010JA015788, 2011.

Tapping, K. F.: Recent solar radio astronomy at centimeter wavelengths: The temporal variability of the 10.7-cm flux, J. Geophys. Res. Atmos., 92, 829–838, https://doi.org/10.1029/JD092iD01p00829, 1987.

Tsurutani, B. T. and Gonzalez, W. D.: The cause of high-intensity long-duration continuous AE activity (HILDCAAs): Interplanetary Alfvén wave trains, Planet. Space Sci., 35, 405–412, https://doi.org/10.1016/0032-0633(87)90097-3, 1987.

https://doi.org/10.5194/angeo-2021-27
Preprint. Discussion started: 24 June 2021

395 Tsurutani, B. T., Gonzalez, W. D., Tang, F., and Lee, Y. T.: Great magnetic storms, Geophys. Res. Lett., 19, 73–76, https://doi.org/10.1029/91GL02783, 1992.

Tsurutani, B. T., Gonzalez, W. D., Guarnieri, F., Kamide, Y., Zhou, X., and Arballo, J. K.: Are high-intensity long-duration continuous AE activity (HILDCAA) events substorm expansion events?, J. Atmos. Sol. Terr. Phys., 66, 167–176, https://doi.org/10.1016/j.jastp.2003.08.015, 2004.

400 Valdés-Galicia, J. F., Pérez-Enríquez, R., and Otaola, J. A.: The Cosmic-Ray 1.68-Year Variation: a Clue to Understand the Nature of the Solar Cycle?, Sol. Phys., 167, 409–417, https://doi.org/10.1007/BF00146349, 1996.

von Humboldt, A.: Die vollständigste aller bisherigen Beobachtungen über den Einfluss des Nordlichts auf die Magnetnadel angestellt, Ann. Phys., 29, 425–429, https://doi.org/10.1002/andp.18080290806, 1808.

Wang, H. and Lühr, H.: Seasonal-longitudinal variation of substorm occurrence frequency: Evidence for ionospheric control, Geophys. Res.
405 Lett., 34, L07 104, https://doi.org/10.1029/2007GL029423, 2007.